Renewable and Sustainable Energy Reviews 38 (2014) 706–716

Contents lists available at ScienceDirect

Renewable and Sustainable Energy Reviews

journal homepage: www.elsevier.com/locate/rser

# The near future availability of photovoltaic energy in Europe and Africa in climate-aerosol modeling experiments

Marco Gaetani [a,*], Thomas Huld [b], Elisabetta Vignati [a], Fabio Monforti-Ferrario [b], Alessandro Dosio [a], Frank Raes [a]

[a] European Commission Joint Research Centre, Institute for Environment and Sustainability, Via E. Fermi 2749, I-21027 Ispra, Italy
[b] European Commission Joint Research Centre, Institute for Energy and Transport, Via E. Fermi 2749, I-21027 Ispra, Italy

ARTICLE INFO

*Article history:*
Received 19 February 2014
Received in revised form
6 May 2014
Accepted 6 July 2014
Available online 24 July 2014

*Keywords:*
Climate model
Climate change
Photovoltaic energy
Europe
Africa
Aerosols

ABSTRACT

The near future change in productivity of photovoltaic energy (PVE) in Europe and Africa is assessed by using the climate variables simulated by the ECHAM5-HAM aerosol-climate model, and a model for the performance of photovoltaic systems. The climate simulations are forced by green-house gases emissions from the IPCC SRES B2 scenario. In addition, different scenarios for future anthropogenic aerosols emissions are applied. Thus, the sensitivity of the future PVE productivity to changes in aerosol atmospheric burdens between 2000 and 2030 is analyzed. The analysis indicates that reductions in aerosols emissions in the near future result in an increase of global warming, and a significant response in surface solar radiation and associated PVE productivity. A statistically significant reduction in PVE productivity up to 7% is observed in eastern Europe and northern Africa, while a significant increase up to 10% is observed in western Europe and eastern Mediterranean. The changes in surface solar radiation and PVE productivity are related to global effects of aerosols reduction on the large scale circulation and associated cloud cover pattern, rather than to local effects on the atmospheric optical properties. PVE assessment is then discussed in the frame of the present situation and next decades evolution of the photovoltaic market, highlighting that the effects on productivity induced by industrial and public policies, and technological development are comparable to climate related effects. The presented results encourage the improvement and further use of climate models in assessment of future renewable energies availability.



**Contents**



* Correspondence to: European Commission Joint Research Centre, Institute for Environment and Sustainability, Climate Risk Management Unit, Via E. Fermi 2749, TP124, I-21027 Ispra, Italy. Tel.: +39 0 332 78 6485.
*E-mail address:* marco.gaetani@jrc.ec.europa.eu (M. Gaetani).

http://dx.doi.org/10.1016/j.rser.2014.07.041

## 1. Introduction

The nexus between renewable energies (RE) and climate has been often investigated in the perspective of the impact on global climate deriving from an increased penetration of renewable sources in the world energy mix, and the associated reduction in carbon dioxide emissions [1,2]. The possibility of fully replacing the pre-existing energy with RE by 2050 has been explored [3,4], suggesting that the barriers to the development of such a plan are primarily social and political [5]. On the other hand, technological and economic limits to high penetration of RE in the electric power system still exist [6], mostly concerning the grid flexibility and energy storage required to incorporate electricity generation from intermittent sources into the transmission grid [7,8]. Nevertheless, the nexus has a second direction too, as climate change is also expected to act on the meteorological variables ultimately governing the availability and geographical location of several renewable resources. Scientific literature on this topic is relatively scarce, and the IPCC itself has pointed out that "Climate change will have impacts on the size and geographic distribution of the technical potential for Renewable Energy sources, but research into the magnitude of these possible effects is nascent" [1].

Among RE resources, electricity generated by solar photovoltaic modules is showing a fast growth, with an expected capacity of 135 GW to be installed by the end of 2013 worldwide [9]. With such expectations and consequent investments being mobilized by the photovoltaic sector, it makes sense to analyze how and to what extent the current photovoltaic potential could be affected in the next decades by the expected changes in the climate patterns, in terms of both energy output and infrastructure vulnerability [10]. However, despite the growing interest, only few studies have investigated directly the impact of climate change on photovoltaic energy production, compared with other renewable sources as hydro and wind power [11]. Some studies, based on climate models projections, estimate by the end of 21st century no or slight increase in Europe [12–14], few percent increase in China [15], and few percent decrease in western USA and Saudi Arabia [15].

The photovoltaic energy (PVE) productivity is related to solar radiation and temperature at the surface of the photovoltaic modules. Solar radiation and temperature are in turn affected by the optical properties of the atmosphere, and in particular, to its aerosols content. Indeed, aerosols interact directly with the solar radiation through scattering and absorption [16], and lead to temperature changes with consequent evaporation of cloud droplets [17]. Moreover, aerosols affect the cloud properties, enhancing cloud albedo by means of an increase in the number of cloud droplets [18], and prolonging cloud lifetime through the formation of smaller droplets which lower the precipitation probability [19].

Understanding the chemistry and dynamics of the aerosols, and their inclusion in climate models, are fundamental steps to improve the description of climate variability [20]. In the context of climate change, a realistic simulation of the observed increasing temperature trend over the 20th century is possible only considering the combined impact of anthropogenic green-house gases (GHG) and aerosol emissions [21]. In particular, a reliable assessment of climate change in the near term, i.e., the next 20–30 years, requires climate models capable of correctly including the role of aerosols, because of the short atmospheric lifetime of aerosols, and because the emissions of aerosols and aerosols precursors are nowadays more effectively regulated than GHG [22–24]. The near term climate change and the role of aerosols are particularly relevant for the assessment of future PVE resources, in which exploitation is based on technologies with 20–30 years lifetime [25,26], and strongly affected by the radiative properties of the atmosphere. As an example, the global abatement of the anthropogenic aerosols emissions is expected to produce a radiative forcing up to around 3 $W/m^2$ at the top of the atmosphere over European Union [22], and this forcing may triple at the surface [27], which equals around 6–9% of the yearly electricity generated in the European Union countries by a typical photovoltaic system [28].

The objective of this work is to assess the near future (2030) availability of PVE in Europe and Africa, with a focus on the sensitivity of PVE resources to different concentrations of anthropogenic aerosols. PVE is estimated through a model for photovoltaic performance which uses as input the solar radiation and air temperature data from a state-of-the-art aerosol-climate model. The effect of the aerosols concentrations on PVE is evaluated by performing climate simulations under different future emission scenarios of anthropogenic aerosols and aerosol precursors.

The paper is structured as follows: the aerosol-climate model, the emission scenarios, the experimental setup, and the photovoltaic performance model are detailed in Section 2; the near future climate simulations and PVE assessment are presented in Section 3; the relationship between PVE availability and the current and expected photovoltaic market risks and opportunities is discussed in Section 4; conclusions are drawn in Section 5.

## 2. Data and methodology

### 2.1. The ECHAM5-HAM aerosol-climate model

The ECHAM5-HAM modeling system is based on the atmospheric general circulation model ECHAM5 [29] coupled to a mixed layer ocean model [30], and extended by the microphysical aerosol model HAM [31] and a cloud scheme with a prognostic treatment of cloud droplet and ice crystal number concentration [32].

ECHAM5 solves the prognostic variables (vorticity, divergence, surface pressure, temperature, water vapor, cloud liquid water, and cloud ice) on a T63 horizontal grid (about 1.8° on a Gaussian Grid), and 31 vertical levels from the surface up to 10 hPa. Fractional cloud cover is predicted from relative humidity according to Sundquist et al. [33]. The shortwave radiation scheme includes 6 bands in the visible and ultraviolet [34].

The microphysical aerosol module HAM predicts the evolution of an ensemble of interacting aerosol modes and is composed of the microphysical core M7 [35]; an emission module for $SO_2$, black and organic carbon, and mineral dust particles; a sulfur oxidation chemistry scheme using prescribed oxidant concentrations for OH, $NO_2$, $O_3$ and $H_2O_2$ [36]; a deposition module; and a module defining the aerosol radiative properties. The HAM module treats the aerosol size distribution, mixing state, and composition as prognostic variables. The aerosol optical properties are explicitly simulated within the framework of the Mie theory, and provided as input for the radiation scheme in ECHAM5 [31]. The model simulates interactively climate sensitive natural emissions such as dimethyl sulfide, sea salt, and dust emissions.

### 2.2. Emission scenarios

GHG concentrations used in the numerical experiments are taken from the IMAGE 2.2 implementation of the SRES B2 scenario [37]. The SRES B2 storyline describes a world with intermediate population and economic growth, in which the emphasis is on local solutions to economic, social, and environmental sustainability.

The anthropogenic emissions of carbonaceous aerosols, namely black carbon (BC) and organic carbon (OC), and sulfur dioxide ($SO_2$), the main precursor of sulfate aerosols, are extracted from an aerosol emission inventory developed by the International Institute for Applied System Analysis. Two possible future developments are considered: current legislation (CLE) and maximum feasible reduction (MFR) [38]. CLE assumes the full compliance of the presently decided control legislations for future developments, while MFR assumes the full implementation of the most advanced available technologies. These scenarios are built using the projection of human activity level (industrial production, fuel consumption, livestock numbers, crop farming, waste treatment and disposal) based on current national perspectives on the economic and energy development up to 2030, in regions where data are available. Elsewhere, the economic and energy future trends estimated in the IPCC SRES B2 MESSAGE scenario [39,40] are considered. Biomass burning emissions, both of anthropogenic and natural origin, are assumed as for 2000. Finally, changes in land use are not taken into account.

### 2.3. Experimental setup

The climate simulations analyzed in this study have been performed by Kloster et al. [22], and in the framework of the FP6-EUCAARI project [41]. The near future changes in climate and PVE are assessed by analyzing the differences between the year 2030 and the present-day (year 2000) conditions reproduced in climate equilibrium simulations. A 100-yr control simulation is performed with present day (year 2000) GHG concentrations, aerosol and aerosol precursor emissions. Three 60-yr sensitivity experiments are performed for the year 2030, using GHG concentrations from the SRES B2 scenario, and three different combinations of aerosols emissions scenarios: (1) in the 2030GHG experiment, aerosols emissions are kept at the 2000 level; (2) in the 2030CLEMFR experiment, MFR is assumed in continental Europe and CLE elsewhere; (3) in the 2030MFR experiment, MFR is assumed worldwide. The 2030GHG experiment, in which only GHG concentrations change, while the emissions of aerosols and aerosols precursors remain at the year 2000 level, is performed to disentangle the effects of changes in GHG concentrations. The experimental setups, along with the 2030–2000 differences in the global averages of the anthropogenic aerosols emissions, are summarized in Table 1.

The climate simulations are analyzed after the model reaches an equilibrium state. To this aim, only the last 60 and 30 years are used in the control and sensitivity experiments to compute annual averages. The statistical significance of the simulated differences is measured by a Student's *t*-test at 95% level of confidence.

### 2.4. ECHAM5-HAM evaluation

The ECHAM5-HAM capability in correctly reproducing climate variables, radiative balance, and aerosol dynamics has been assessed and validated in several studies [22,23,31,42,43]. However, a brief evaluation of the model is presented in the Supplementary material online (Section S1) for the climate variables which are relevant to the PVE assessment, namely surface solar radiation (SSR), 2-meter air temperature (*T*2), and total cloud cover (TCC, defined as the grid-box fraction covered by clouds). *T*2 is used to represent temperature at the surface of the photovoltaic modules, which affects negatively PVE productivity reducing the performance by 0.5% for every 1 K increase [10]. TCC is also important in the PVE assessment for its strong negative relationship with SSR [44,45].

ECHAM5-HAM shows generally small biases in reproducing the observed climate drivers for the photovoltaic performance model in Europe and Africa. Specifically, significant *T*2 differences are around 1 K, with few isolated locations in eastern Equatorial Africa and Scandinavia reaching 2 K or higher differences, while significant SSR differences peak at 30–40 $W/m^2$, corresponding to 10–20% of the observed SSR. However, the absolute bias in the drivers is less relevant, as the objective of this analysis is the response of the photovoltaic performance model to the future changes in the climate drivers, with a specific focus on the role of the anthropogenic aerosols emissions.

### 2.5. Photovoltaic performance model

The photovoltaic performance model used in this study integrates climate variables in a model for inclined-plane irradiation and photovoltaic system output [28,46–48]. The photovoltaic modules are assumed to be mounted in a fixed position, facing equator, and at the local optimum angle for maximum yearly energy yield [48]. The effect of module temperature and irradiance on photovoltaic module efficiency is accounted for by using the model presented in Huld et al. [49,50], which includes the effects of shallow-angle reflectance [51], while other losses in the system (e.g., inverter losses, resistive losses in cables) are assumed to remain constant. The effect of snow and dust cover is not included in the calculation. For the present calculation, the modules are assumed to use crystalline silicon photovoltaic cells, the most prevalent photovoltaic module type nowadays. PVE productivity is computed for a typical day in the month, by using the monthly averages of global and diffuse horizontal irradiation, and daytime temperatures at the surface of the modules.

As diffuse irradiation is not a direct output variable of ECHAM5-HAM, its estimate is necessary before using it in the photovoltaic performance model. The key assumption is that the percentage of diffuse irradiation, *R*, remains constant in different climates, that is

$$R = D/G = \text{const}$$

where *D* and *G* are the monthly diffuse and global irradiation, respectively. This assumption is possible because the computation of irradiation on an inclined plane is not strongly dependent on *R*,

**Table 1**
ECHAM5-HAM experimental setup and references, and 2030–2000 percentage differences in the global anthropogenic aerosols emissions.

| Experiment | GHG | Aerosols emissions | 2030–2000 Emissions change | | | References |
|---|---|---|---|---|---|---|
| | | | BC | $SO_2$ | OC | |
| 2000 | 2000 | 2000 | | | | [22] |
| 2030GHG | 2030 | 2000 | | | | [22] |
| 2030CLEMFR | 2030 | 2030 CLE worldwideand MFR in Europe | −13% | +1% | −8% | [41,43] |
| 2030MFR | 2030 | 2030 MFR | −27% | −42% | −12% | [22,43] |

and the error can be considered negligible. The discussion of using constant monthly $R$ is beyond the scope of this manuscript, however more details can be found in the Supplementary material online (Section S2). For the present study, $R$ is estimated from irradiation data derived from the SEVIRI and GERB instruments on board the Meteosat Second Generation satellites [52,53], thus the diffuse irradiation for ECHAM5-HAM simulations, $D_S$, can be computed by using SSR as an estimation of $G$, so that

$$D_S = R \cdot \mathrm{SSR}.$$

The photovoltaic performance model uses the daytime temperature profile, which is approximated with a 3rd order polynomial

$$T(t) = k_3 t^3 + k_2 t^2 + k_1 t + k_0,$$

where $T$ is the temperature at time $t$. The coefficients $k_n$ can be estimated through a linear fit of the monthly means of temperature at sub-daily steps. Since the ECHAM5-HAM time step is 6 h, three daytime values (at 6:00, 12:00, and 18:00) are not enough to solve the above linear system; therefore the daytime temperature profiles in the numerical experiments are estimated from observations. For the present-day simulation, it is assumed that the difference between observed and simulated temperature remains constant during daytime, so that the profile is unchanged. Similarly, for future climate it is assumed that the temperature change related to global warming affects all times of the day equally. Therefore, the daytime temperature profile in the climate simulations, $T_S$, is obtained by adding to the observed temperature profile, described by the polynomial expression, the difference, $\Delta T$, between the monthly means of observed and simulated temperature

$$T_S(t) = T(t) + \Delta T = k_3 t^3 + k_2 t^2 + k_1 t + k_0 + \Delta T.$$

The observed daytime temperature profile is computed using data extracted from the ERA-interim data set [54] in the period 2005–2009.

## 3. Results

In this section, the climate variables relevant to the estimation of PVE productivity are analyzed, by comparing the 2030–2000 differences in the three emissions scenarios, and by discussing the dynamical mechanisms explaining the near future changes. The response of PVE productivity to climate change is finally described and discussed in the frame of the evolution of PVE market. The near future PVE assessment is limited to Europe and Africa because of the coverage of the MSG irradiation data [52] needed to compute the diffuse irradiation (see Section 2.5).

### 3.1. Near future climate change

The 2030–2000 difference in $T2$ for the three aerosols emissions scenarios is displayed in Fig. 1. A global significant warming is observed in the three experiments, along with a pronounced north–south inter-hemispheric gradient. The intensity of the global warming is directly related to the aerosols emissions reduction, with an average warming of 1.3 K in the 2030GHG simulation, 1.5 K in the 2030CLEMFR simulation, and 2.5 K in the 2030MFR simulation. Also the inter-hemispheric gradient depends on the emissions scenarios, with the Northern Hemisphere being 0.7 K warmer than the Southern in the 2030GHG experiment, 0.9 K in 2030CLEMFR and 2.0 K in 2030MFR. The increase in global warming and inter-hemispheric thermal gradient (summarized in Table 2) is mainly related to the action of sulfate aerosols on the atmospheric reflectivity of solar radiation, i.e., a reduction in the sulfate aerosols burden results in an atmospheric warming [23].

SSR (Fig. 2) shows significant positive changes in the Tropics, at mid and high latitudes, and negative changes in the sub-Tropics in all the 2030 simulations. The extension and intensity of the simulated changes increase as the aerosols emissions decrease, confirming that the climate change signal related to GHG increase is augmented by the reduction of anthropogenic aerosols emissions. This aspect is widely discussed by Kloster et al. [22,23], who highlighted that a reduction in aerosols emissions, without any intervention on GHG, improves air quality, with a positive impact on human health, but may produce, on the other hand, a strong increase in the global radiative forcing.

SSR variability is primarily driven by cloudiness [44,45], and this is evident when computing the 2030–2000 TCC differences in the three scenarios. The latitudinal distribution of TCC differences displayed in Fig. 3 reflects the SSR pattern in Fig. 2, with reduced (increased) cloudiness over northern sub-Tropics and mid-latitudes, and southern Tropics (northern Tropics) corresponding to increased (reduced) SSR in the same regions.

The simulated changes in cloudiness suggest a future climate characterized by modifications in the atmospheric circulation [55,56]. This hypothesis is verified by further analyzing the 2030MFR experiment, which shows the most intense change compared to the year 2000. The 2030MFR–2000 differences in $T2$, averaged in boreal summer (June–September, JJAS) and winter (December–March, DJFM), present a significant global increase characterized by a north–south inter-hemispheric gradient, with higher values in boreal winter. Specifically, the global increase is 2.1 K in JJAS, and 2.8 K in DJFM, while the north–south gradient is 1.8 K in JJAS, and 3.0 K DJFM (Table 2). The seasonal means of the global warming and inter-hemispheric thermal gradient computed for the 2030GHG and 2030CLEMFR experiments reflect the behavior of the annual means, with increasing values as the aerosols emissions decrease, and the winter values higher than the summer ones (Table 2). The global warming and inter-hemispheric thermal gradient affect the intensity and location of the intertropical convergence zone [57]. In boreal summer, it results in an intensification of the monsoonal regime and associated cloudiness over northern Africa and southern Asia (Fig. 3c), and a strengthening of the Hadley meridional circulation which produces downward vertical motions, and associated subsidence and clear sky conditions at subtropical latitudes [58] (Fig. 3c). In boreal winter, the land–sea thermal gradient in the Northern Hemisphere contrasts the high pressure belt over the American and Eurasian continents with lows over the Atlantic and Pacific oceans, resulting in a modification of the midlatitude atmospheric circulation and associated storm-track (not shown). Specifically, a high-low pressure dipole is forced in the Euro-Atlantic sector, and it orientates the westerly flow toward the Scandinavian peninsula, with a consequent excess of cloudiness over the North Atlantic storm-track (Fig. 3c).

### 3.2. Near future PVE assessment

The year 2000 annual PVE production estimated for Europe and Africa by using the ECHAM5-HAM data into the photovoltaic performance model is presented in Fig. 4. The annual mean is directly related to the solar radiation pattern, showing maxima over the desert areas and minima over the Equatorial belt and mid-latitudes (Fig. 4a), which are characterized by higher cloud cover. The year 2000 PVE production is compared to the production estimated by the photovoltaic performance model from satellite and reanalysis products in the period 1996–2005 (Fig. 4b). Specifically, the solar radiation is retrieved from the Meteosat First Generation satellites [59] and $T2$ data from the ERA-Interim archive.

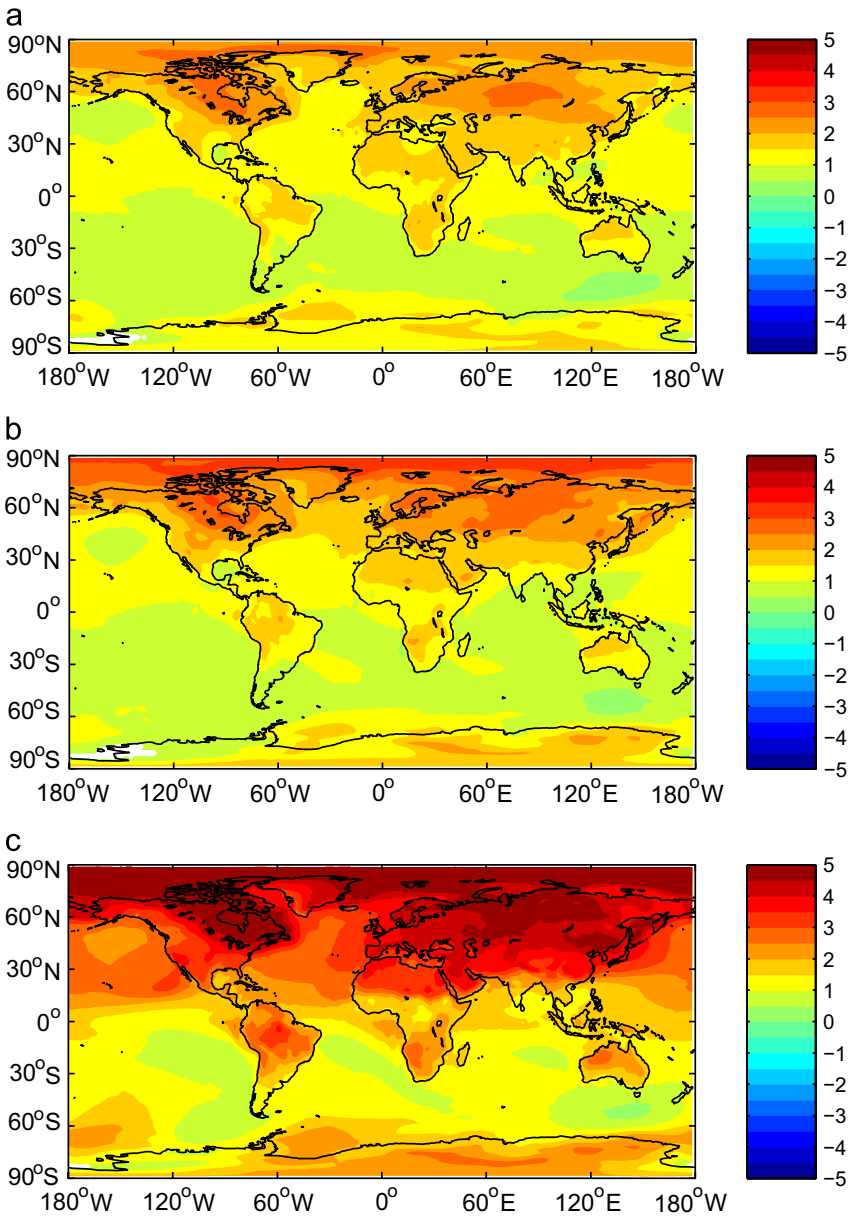


**Fig. 1.** Annual mean of 2-m air temperature [K], 2030–2000 differences in ECHAM5-HAM simulations: (a) 2030GHG–2000, (b) 2030CLEMFR–2000 and (c) 2030MFR–2000. Shadings indicate 95% significant differences.

**Table 2**
2030–2000 global warming and inter-hemispheric thermal gradient [K] in the ECHAM5-HAM experiments.

| Experiment | Annual mean | | JJAS | | DJFM | |
|---|---|---|---|---|---|---|
| | Warming | Gradient | Warming | Gradient | Warming | Gradient |
| 2030GHG | 1.3 | 0.7 | 1.1 | 0.2 | 1.5 | 1.1 |
| 2030CLEMFR | 1.5 | 0.9 | 1.3 | 0.3 | 1.6 | 1.4 |
| 2030MFR | 2.5 | 2.0 | 2.1 | 1.0 | 2.8 | 3.0 |

ECHAM5-HAM shows overestimations in western Asia and northern sub-Tropics, up to around 250 kWh/m$^2$ (corresponding to about 15% of the 'observed' PVE) over the Sahara desert, and underestimations in western Europe and around the Equator, up to around 400 kWh/m$^2$ (about 20% of the 'observed' PVE) in southwestern Europe (Fig. 4b). These errors in the PVE estimation are strongly related to the ECHAM5-HAM bias in describing the observed SSR, though some deviations are observed in central Equatorial Africa, where a strong overestimation of SSR is related to a weak underestimation of PVE.

The response of PVE productivity in Europe and Africa to the different future emissions scenarios is presented in Fig. 5. Significant changes related to the increase of GHG concentrations are observed in the 2030GHG experiment (Fig. 5a). The productivity is reduced in northern Africa (around 3%), and eastern Europe (around 6%), while an increase in the productivity benefits

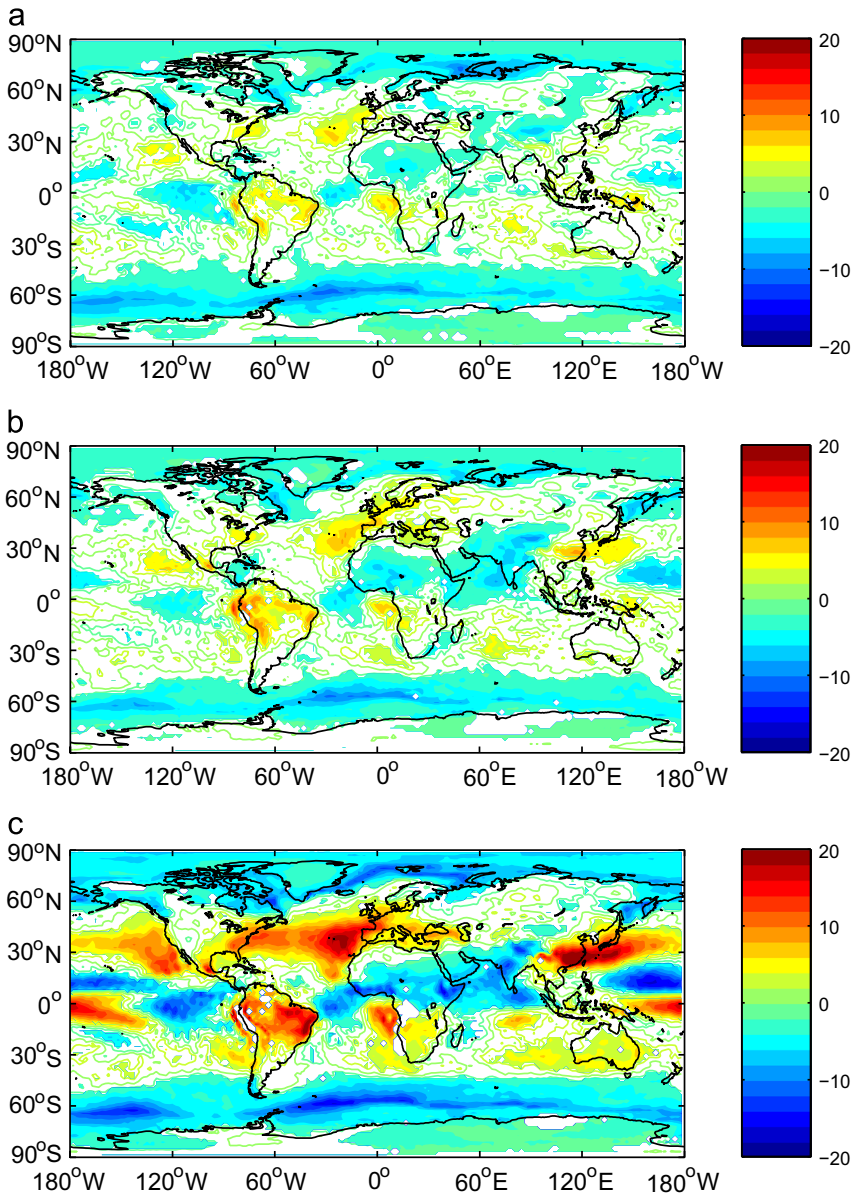


**Fig. 2.** Same as Fig. 1 but for surface solar radiation [W/m$^2$].

southern Tropical Atlantic, and sub-Tropical North Atlantic (around 3%). A similar pattern is observed when the 2030CLEMFR experiment is analyzed (Fig. 5b). Larger differences are observed over northern Africa (up to 4%), sub-Tropical North Atlantic, and western Europe (up to 5%), while the reduction over eastern Europe is not significant. The largest change is observed when the MFR scenario is considered, with expected changes up to 10% (Fig. 5c). Such a strong abatement of aerosols emissions worldwide produces a significant positive response in PVE productivity in southern Tropical Atlantic (up to 6%), eastern Mediterranean (up to 3%), and western Europe (up to 10%). On the other hand, a sizable reduction is observed in northern African continent, with a peak around 6% in the Equatorial belt, and in eastern Europe (up to 7%).

By comparing Fig. 5 to Figs. 1 and 2, the strong relationship between PVE and solar radiation is evident, while the negative effect of the air temperature appears weak [10]. Therefore, the changes in the future PVE productivity may be connected to the modifications, discussed above, in the large scale circulation affecting cloudiness. Thus, the increase in the solar radiation and associated PVE productivity in western Europe and the Mediterranean may be related to the subsidence and consequent reduced cloudiness produced by the strengthening of the Hadley circulation in JJAS, while the concomitant reduction in eastern Europe is related to the cloudiness associated with the storm-track in DJFM (see Section 3.1). A similar relationship between atmospheric circulation over North Atlantic, and SSR in the Euro-Atlantic sector has been already documented by Chiacchio and Wild [55], and Pozo-Vazquez et al. [56]. On the other hand, the solar radiation and PVE decrease in northern Africa is linked to the augmented cloudiness associated with the reinforced monsoonal activity in JJAS.

## 4. PVE assessment in the present and future market and policy context

The changes in PVE productivity, assessed in the previous section for the 2030 time horizon, are discussed in the context

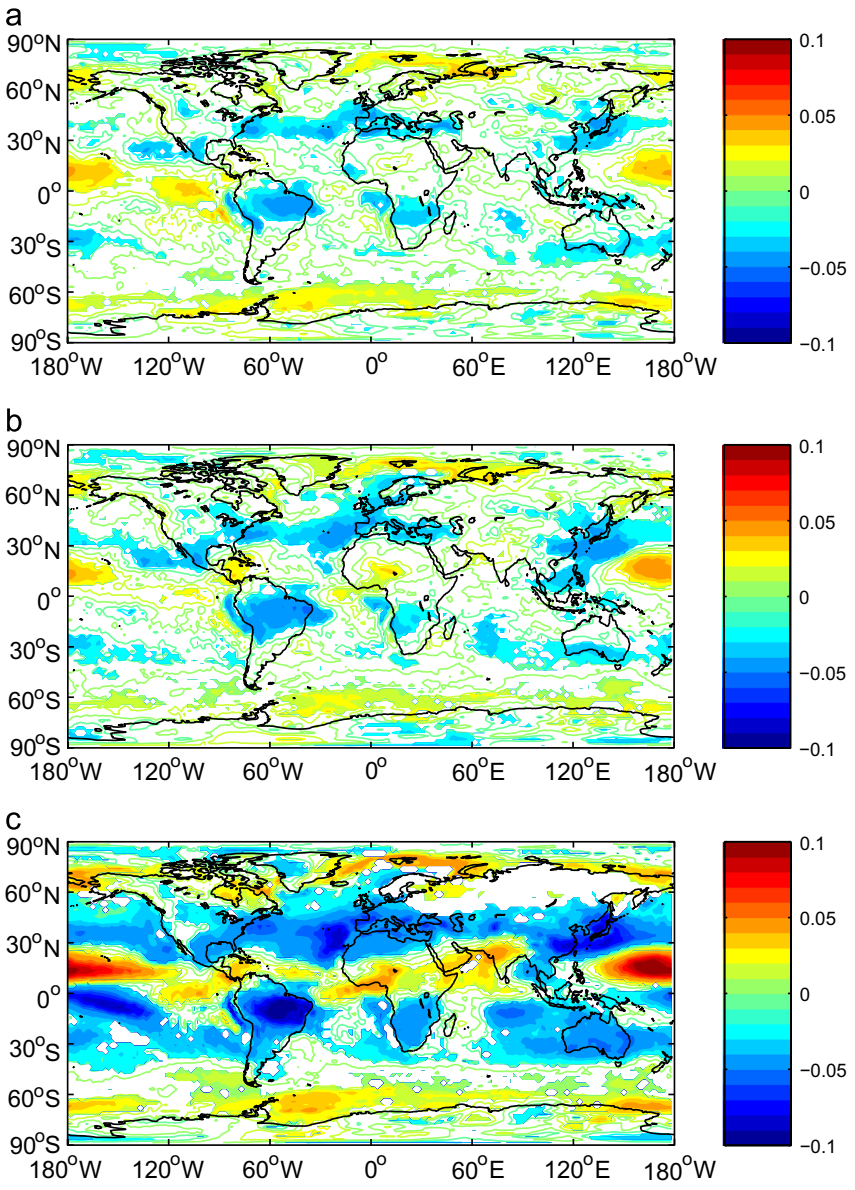


**Fig. 3.** Same as Fig. 1 but for total cloud cover, which is defined as the fraction of the grid-box covered by clouds.

of the current and near future PVE market opportunities. A commonly agreed measure of costs of electricity production is the levelized cost of electricity production (LCOE), which represents the cost at which the electricity should be generated to break even over the lifetime of the project, or, if sold on the market, to provide a given level of return of investment [9]. Factors influencing LCOE are the investment expenditures, and their time pattern, operational and maintenance costs, fuel costs (zero in the case of PVE), electricity generation, discount rate (or costs of capital), and lifetime of the infrastructure.

All the other factors fixed, LCOE is strongly inversely linearly dependent on energy production, but sensitivity analysis shows that factors other than energy production have an influence of the same order of magnitude or even larger if combined together [60]. Such an influence of factors other than energy production is well known, for example, in the case of Europe, where governments act on these non-physical factors in order to induce a decrease of costs by supporting photovoltaic systems deployment. Fig. 6 shows how the geographical distribution of the installed capacities only partially reflects the actual distribution of raw irradiation resources [61]. At least in the case of Europe, appropriate policies have been able to overcome initial discrepancies of the order of even 100% between some southern and central-northern countries, and are expected to be able to compensate the few percent effects described in this paper. Moreover, photovoltaic module costs have shown so far a clear market volume effect that has been estimated to be consistent with a 'rule of thumb' of a module price decrease of about 20% for each doubling of the global photovoltaic installed capacity [9]. According to recent estimates [62], the doubling of photovoltaic world capacity installed in 2013 is expected for 2018, i.e., largely before the time horizon of the climate induced changes investigated in this study.

In conclusion, both industrial and public policies have been shown capable to provide comparable market opportunities for photovoltaic systems in countries with differences in raw resources much larger than the ones expected in next decades from climatic effects. Moreover, technological development foreseen in the time horizon analyzed in this study is expected to induce a decrease of LCOE for PVE larger than possible fluctuations caused by climatic effects. Nevertheless, these conclusions could

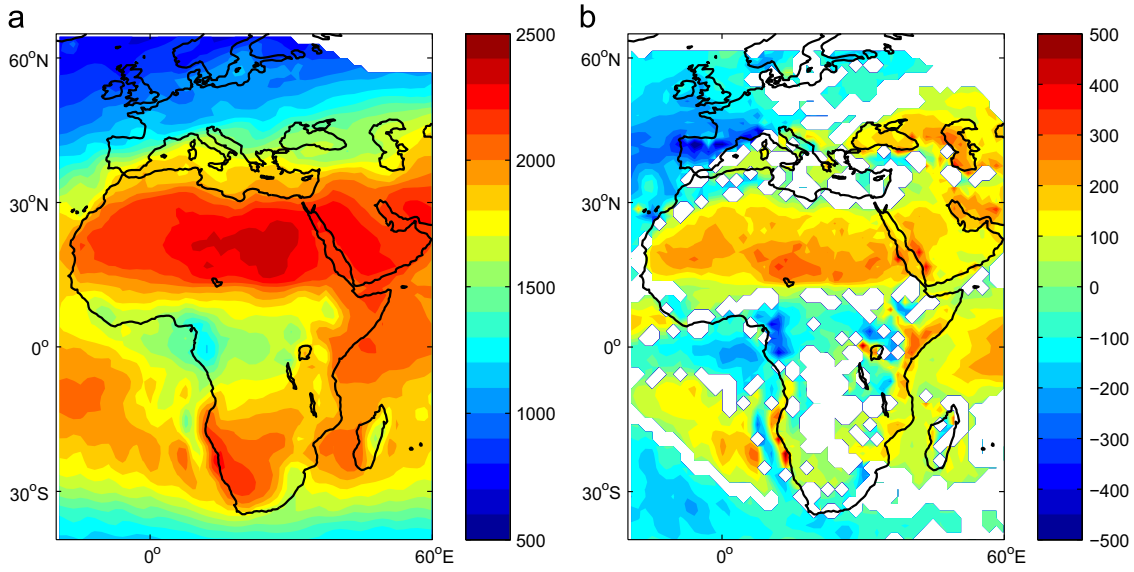


**Fig. 4.** Photovoltaic energy production [kWh/m$^2$]: ECHAM5-HAM (a) year 2000 annual mean and (b) 95% significant differences with estimates based on reanalysis and satellite data for 1996–2005.

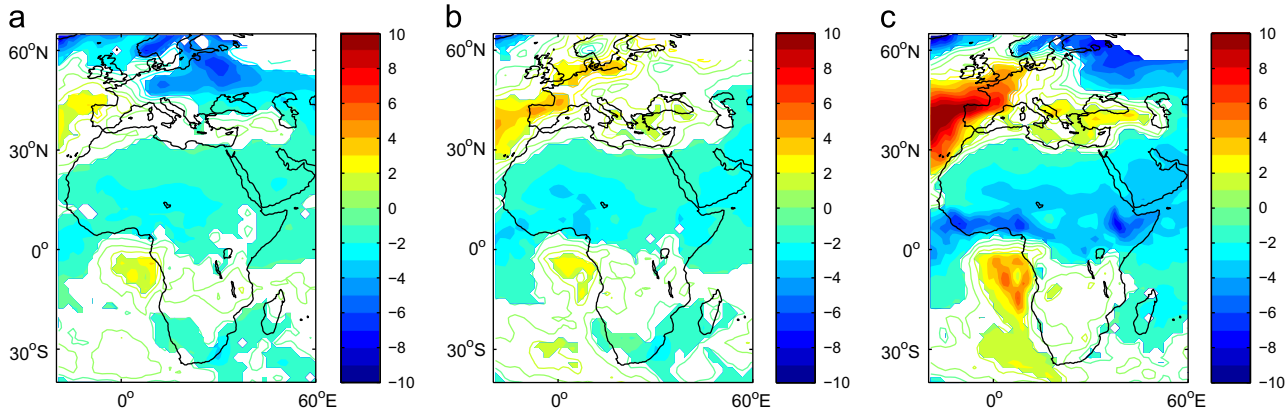


**Fig. 5.** Same as Fig. 1 but for photovoltaic energy production in %.

be less robust if a longer time scale is investigated, where technology learning curves could reach the stability typical of mature technologies and, on the contrary, climatic effects could continue to cumulate.

## 5. Summary and conclusions

In this work the near future (2030) productivity of PVE in Europe and Africa is assessed by integrating climate variables simulated by the ECHAM5-HAM model into a model for the performance of photovoltaic systems. The climate simulations are performed using different scenarios for future aerosols emissions reduction, aiming to evaluate the sensitivity of future PVE availability to the aerosols impact on projected climate change. Results indicate a sizable impact of the aerosols reduction on the future climate change, with an increase in the projected global warming. Specifically, the increase in surface temperature and north–south inter-hemispheric thermal gradient shifts northward and intensifies the Hadley meridional circulation, producing augmented cloudiness and reduced solar radiation over northern Africa, and clear sky and sunny conditions over western Europe and the Mediterranean. Moreover, the land–sea thermal contrast in the Euro-Atlantic sector affects the North Atlantic storm-track favoring storminess and reducing solar radiation over northern and eastern Europe. Thus, a significant response in PVE productivity is observed in 2030, with the strength of the signal directly related to the abatement of anthropogenic aerosols. Specifically, a reduction in PVE productivity is observed in eastern Europe, and northern Africa (up to 7% in the MFR scenario), while an increase is observed in western Europe, and eastern Mediterranean (up to 10% in the MFR scenario). These results are consistent with the findings by Crook et al. [15], who used the HadGEM1 and HadCM3 climate models under the IPCC SRES A1B scenario [63] to examine how the projected changes in temperature and insolation over the 21st century will affect photovoltaic productivity. They found that photovoltaic output is likely to increase by a few percent in Europe and China, and decrease by a few percent in western USA and Saudi Arabia.

The presented results demonstrate that climate modeling is a valuable tool for investigating the future changes in PVE productivity. Indeed, PVE productivity shows sensitivity to the simulation of different future scenarios, and a coherent relationship with the projected future modifications in the climate dynamics. Therefore, though market flexibility and technological development are likely to overcome any potential risk and benefit coming from climate driven changes in PVE productivity in the time horizon analyzed in the present study, this paper encourages a broader use of climate

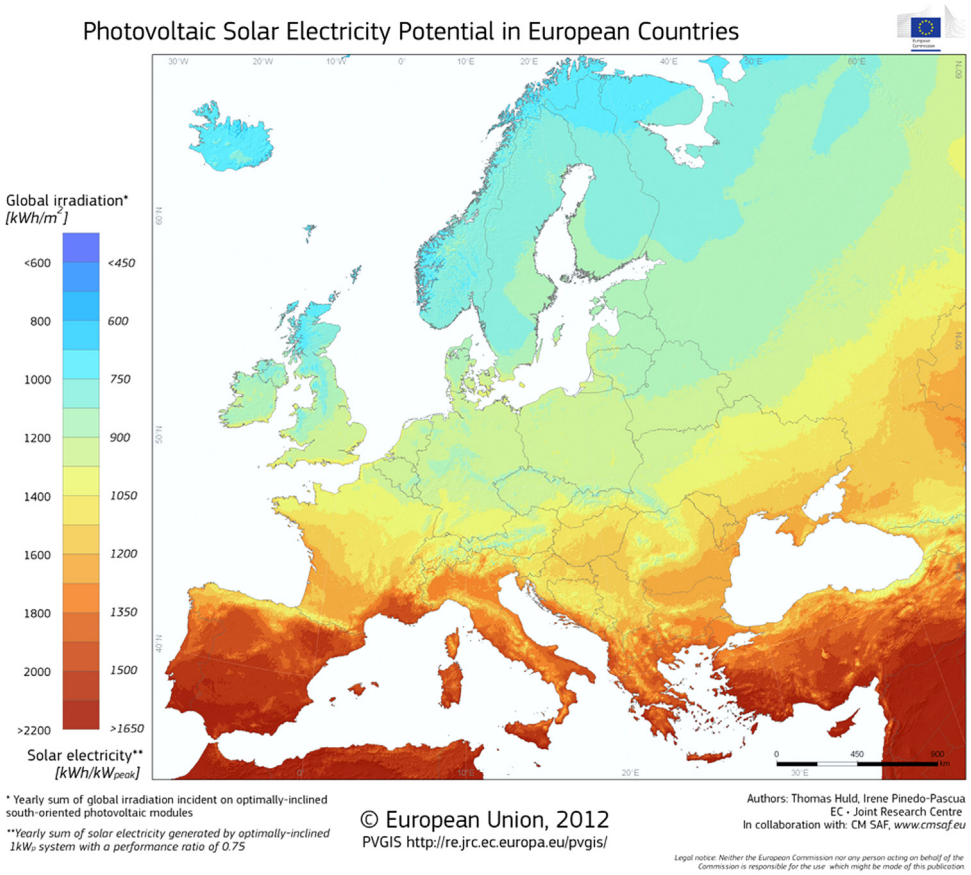


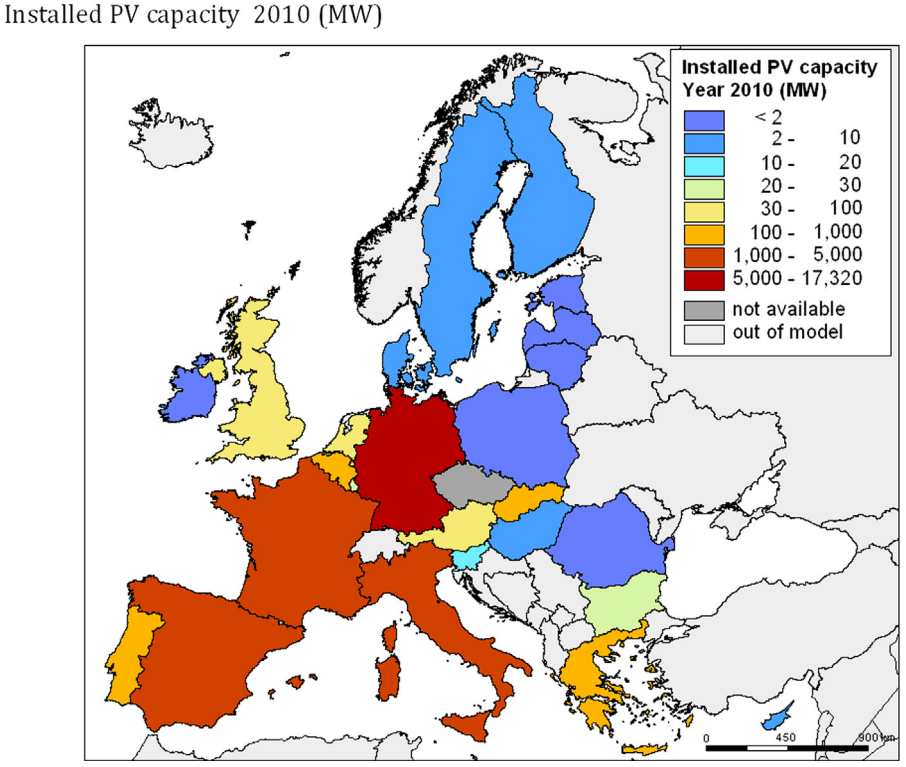


**Fig. 6.** Top panel: solar irradiation and potential electricity production [28,48]. Bottom panel: PV installed capacity in EU-27 in 2010 [61].

models in the assessment of RE future availability. Moreover, an improvement of the climate simulations features specific to RE applications, e.g., the explicit computation of the diffuse irradiation for photovoltaic performance models, would be desirable. The importance of the air quality policy options in the future climate change, and specifically for the future PVE productivity is also highlighted. In this respect, the use of a state-of-the-art aerosol-climate model can be considered the added value of this

study. Indeed, the inclusion of the aerosols dynamics in climate simulations is crucial for a correct assessment of the climate signal and related PVE productivity, because of the impact of the aerosols on the atmospheric dynamics and radiative balance.

## Acknowledgments

This work has been carried out in the framework of the Exploratory Research Project "Climate modeling and renewable energy resource assessment" funded by European Commission Joint Research Centre. Authors wish to thank L. Pozzoli and S. Kloster for running the numerical experiments used in this study, K. Bodis for production of Fig. 6, and A. Jäger-Waldau for useful discussions.

## Appendix A. Supplementary materials

Supplementary data associated with this article can be found in the online version at http://dx.doi.org/10.1016/j.rser.2014.07.041.

## References

[1] Intergovernmental Panel on Climate Change. Special report on renewable energy sources and climate change mitigation, summary for policymakers. Cambridge: Cambridge University Press; 2011.
[2] United Nations. Economic Commission for Africa. Integrating renewable energy and climate change policies: exploring policy options for Africa. Working paper no. 10. UNECA African Climate Policy Centre; 2011.
[3] Jacobson MZ, Delucchi MA. Providing all global energy with wind, water, and solar power, Part I: technologies, energy resources, quantities and areas of infrastructure, and materials. Energy Policy 2011;39:1154–69.
[4] Delucchi MA, Jacobson MZ. Providing all global energy with wind, water, and solar power, Part II: reliability, system and transmission costs, and policies. Energy Policy 2011;39:1170–90.
[5] Jacobson MZ, Archer CL. Saturation wind power potential and its implications for wind energy. Proc Natl Acad Sci 2012;109:15679–84.
[6] European Climate Foundation. Roadmap 2050: a practical guide to a prosperous, low-carbon Europe. The Hague, Netherlands: European Climate Foundation; 2010.
[7] Denholm P, Ela E, Kirby B, Milligan M. Role of energy storage with renewable electricity generation. Report TP-6A2-47187. National Renewable Energy Laboratory; 2010.
[8] Denholm P, Hand M. Grid flexibility and storage required to achieve very high penetration of variable renewable electricity. Energy Policy 2011;39:1817–30.
[9] Jäger-Waldau A. PV status report 2013. Luxembourg: Publication Office of the European Union; 2013, EUR 26118 EN.
[10] Patt A, Pfenninger S, Lilliestam J. Vulnerability of solar energy infrastructure and output to climate change. Clim Change 2013;121:93–102.
[11] Schaeffer R, Szklo AS, de Lucena AFP, BSMC Borba, LPP Nogueira, Fleming FP, et al. Energy sector vulnerability to climate change: a review. Energy 2012;38:1–12.
[12] Pasicko R, Brankovic C, Simic Z. Assessment of climate change impacts on energy generation from renewable sources in Croatia. Renew Energy 2012;46:224–31.
[13] Wachsmuth J, Blohm A, Gößling-Reisemann S, Eickemeier T, Ruth M, Gasper R, et al. How will renewable power generation be affected by climate change? The case of a Metropolitan Region in Northwest Germany Energy 2013;58:192–201.
[14] Dowling P. The impact of climate change on the European energy system. Energy Policy 2013;60:406–17.
[15] Crook JA, Jones LA, Forstera PM, Crook R. Climate change impacts on future photovoltaic and concentrated solar power energy output. Energy Environ Sci 2011;4:3101–9.
[16] Angstroem A. Atmospheric turbidity, global illumination and planetary albedo of the earth. Tellus 1962;14:435–50.
[17] Hansen J, Sato M, Ruedy R. Radiative forcing and climate response. J Geophys Res 1997;102:6831–64.
[18] Twomey S. The influence of pollution on the shortwave albedo of clouds. J Atmos Sci 1977;34:1149–52.
[19] Albrecht BA. Aerosols, cloud microphysics, and fractional cloudiness. Science 1989;245:1227–30.
[20] Heintzenberg J, Raes F, Schwartz SE. Tropospheric aerosols. In: Brasseur G, Prinn RG, Pszenny AAP, editors. Atmospheric chemistry in a changing world, an integration and synthesis of a decade of tropospheric chemistry research. Berlin: Springer; 2003. p. 125–56.
[21] Roeckner E, Bengtsson L, Feichter J, Lelieveld J, Rodhe H. Transient climate change simulations with a coupled atmosphere-ocean GCM including the tropospheric sulfur cycle. J Clim 1999;12:3004–32.
[22] Kloster S, Dentener F, Feichter J, Raes F, van Aardenne J, Roeckner E, et al. Influence of future air pollution mitigation strategies on total aerosol radiative forcing. Atmos Chem Phys 2008;8:6405–37.
[23] Kloster S, Dentener F, Feichter J, Raes F, Lohmann U, Roeckner E, et al. GCM study of future climate response to aerosol pollution Reductions. Clim Dyn 2010;34:1177–94.
[24] Raes F, Seinfeld JH. New directions: climate change and air pollution abatement: a bumpy road. Atmos Environ 2009;43:5132–3.
[25] Skoczek A, Sample T, Dunlop ED. The results of performance measurements of field-aged crystalline silicon photovoltaic modules. Prog Photovolt Res Appl 2009;17:227–40.
[26] Jordan DC, Kurtz SR. Photovoltaic degradation rates – an analytical review. Prog Photovolt Res Appl 2013;21:12–29.
[27] Ramanathan V, Carmichael G. Global and regional climate changes due to black carbon. Nat Geosci 2008;1:221–7.
[28] Suri M, Huld T, Dunlop ED, Ossenbrink H. Potential of solar electricity generation in the European Union member states and candidate countries. Sol Energy 2007;81:1295–305.
[29] Roeckner E, Baeuml G, Bonventura L, Brokopf R, Esch M, Giorgetta M, et al. The atmospheric general circulation model ECHAM5, Part I: model description. Report 349. Hamburg: Max Planck Institute for Meteorology; 2003.
[30] Roeckner E, Siebert T, Feichter J. Climatic response to anthropogenic sulfate forcing simulated with a general circulation model. In: Charlson RJ, Heintzenberg J, editors. Aerosol forcing of climate. New York: John Wiley & Sons Ltd.; 1995.
[31] Stier P, Feichter J, Kinne S, Kloster S, Vignati E, Wilson J, et al. The aerosol-climate model ECHAM5-HAM. Atmos Chem Phys 2005;5:1125–56.
[32] Lohmann U, Stier P, Hoose C, Ferrachat S, Kloster S, Roeckner E, et al. Cloud microphysics and aerosol indirect effects in the global climate model ECHAM5-HAM. Atmos Chem Phys 2007;7:3425–46.
[33] Sundquist H, Berge E, Kristiansson JE. Condensation and cloud parameterization studies with a mesoscale numerical weather prediction model. Mon Weather Rev 1989;117:1641–57.
[34] Cagnazzo C, Manzini E, Giorgetta MA, PMDF Forster, Morcrette JJ. Impact of an improved shortwave radiation scheme in the MAECHAM5 general circulation model. Atmos Chem Phys 2007;7:2503–15.
[35] Vignati E, Wilson J, Stier P. M7: a size resolved aerosol mixture module for the use in global aerosol models. J Geophys Res 2004;109:D22202.
[36] Feichter J, Kjellstrom E, Rodhe H, Dentener F, Lelieveld J, Roelofs GJ. Simulation of the tropospheric sulfur cycle in a global climate model. Atmos Environ 1996;30:1693–707.
[37] European Environment Agency. The IMAGE 2.2 implementation of the SRES scenarios: a comprehensive analysis of emissions, climate change and impacts in the 21st century. Bilthoven: RIVM National Institute for Public Health and the Environment; 2001 (CD-ROM publication 481508018).
[38] Cofala J, Amann M, Klimont Z, Kupiainen K, Hglund-Isaksson L. Scenarios of global anthropogenic emissions of air pollutants and methane until 2030. Atmos Environ 2007;41:8486–99.
[39] Riahi K, Roehl R. Greenhouse gas emissions in a dynamics-as-usual scenario of economic and energy development. Technol Forcast Soc Change 2005;63:175–205.
[40] Nakicenovic N, Alcamo J, Davis G, de Vries HJM, Fenhann J, Gaffin S, et al. Special report on emissions scenarios. Cambridge: Cambridge University Press; 2000.
[41] Kulmala M, Asmi A, Lappalainen HK, Baltensperger U, Brenguier JL, Facchini MC, et al. General overview: European Integrated project on Aerosol Cloud Climate and Air Quality interactions (EUCAARI), integrating aerosol research from nano to global scales. Atmos Chem Phys 2011;11:13061–143.
[42] Fischer-Bruns I, Feichter J, Kloster S, Schneidereit A. How present aerosol pollution from North America impacts North Atlantic climate. Tellus 2010;62A:579–89.
[43] Sillmann J, Pozzoli L, Vignati E, Kloster S, Feichter J. Aerosol effect on climate extremes in Europe under different future scenarios. Geophys Res Lett 2013;40:2290–5.
[44] Chiacchio M, Vitolo R. Effect of cloud cover and atmospheric circulation patterns on the observed surface solar radiation in Europe. J Geophys Res 2012;117:D18207.
[45] Bartok B. Changes in solar energy availability for south-eastern Europe with respect to global warming. Phys Chem Earth 2010;35:63–9.
[46] Suri M, Hofierka J. A new GIS-based solar radiation model and its application to photovoltaic assessment. Trans GIS 2004;8:175–90.
[47] Suri M, Huld T, Dunlop ED. PV-GIS: a web-based solar radiation database for the calculation of PV potential in Europe. J Sustain Energy 2005;24:55–67.
[48] Huld T, Muller R, Gambardella A. A new solar radiation database for estimating PV performance in Europe and Africa. Sol Energy 2012;86:1803–15.
[49] Huld T, Gottschalg R, Beyer HG, Topic M. Mapping the performance of PV modules, effects of module type and data averaging. Sol Energy 2010;84:324–338.
[50] Huld T, Friesen G, Skoczek A, Kenny R, Sample T, Field M, et al. A power-rating model for crystalline silicon PV modules. Sol Energy Mater Sol Cells 2011;95:3359–69.
[51] Martin N, Ruiz JM. Calculation of the PV modules angular losses under field conditions by means of an analytical model. Sol Energy Mater Sol Cells 2001;70:25–38.
[52] Schmetz J, Pili P, Tjemkes S, Just D, Kerkmann J, Rota S, et al. An introduction to Meteosat Second Generation (MSG). Bull Am Meteorol Soc 2002;83:977–992.

[53] Mueller R, Matsoukas C, Gratzki A, Behr H, Hollmann R. The CM-SAF operational scheme for the satellite based retrieval of solar surface irradiance – a LUT based eigenvector hybrid approach. Remote Sens Environ 2009;113:1012–24.
[54] Dee DP, Uppala SM, Simmons AJ, Berrisford P, Poli P, Kobayashi S, et al. The ERA-Interim reanalysis: configuration and performance of the data assimilation system. Q J R Meteorol Soc 2011;137:553–97.
[55] Chiacchio M, Wild M. Influence of NAO and clouds on longterm seasonal variations of surface solar radiation in Europe. J Geophys Res 2010;115:D00D22.
[56] Pozo-Vázquez D, Tovar-Pescador J, Gámiz-Fortis SR, Esteban-Parra MJ, Castro-Díez Y. NAO and solar radiation variability in the European North Atlantic region. Geophys Res Lett 2004;31:L05201.
[57] Biasutti M, Giannini A. Robust Sahel drying in response to late 20th century forcings. Geophys Res Lett 2006;33:L11706.
[58] Fontaine B, Roucou P, Gaetani M, Marteau R. Recent changes in precipitation, ITCZ convection and northern tropical circulation over North Africa (1979–2007). Int J Climatol 2011;31:633–48.
[59] Posselt R, Mueller R, Stöckli R, Trentmann J. Remote sensing of solar surface radiation for climate monitoring, the CM-SAF retrieval in international comparison. Remote Sens Environ 2012;118:186–98.
[60] Kost C, Schlegl T, Thomsen J, Nold S, Mayer J. Levelized cost of electricity for renewable energies. Fraunhofer Insistut for Sol Energy Syst 2012.
[61] Banja M, Scarlat N, Monforti F. Renewable energy development in EU-27 (2009–2010). Luxembourg: Publication Office of the European Union; 2013, EUR 26166 EN.
[62] International Energy Agency. Renewable energy 2013, medium-term market report, market trends and projections to 2018. Paris: IEA Publication Office; 2013.
[63] Intergovernmental Panel on Climate Change. Climate change 2007: the physical science basis, contribution of working group I to the fourth assessment report of the IPCC. Cambridge: Cambridge University Press; 2007.